JOURNAL OF X-RAY SCIENCE AND TECHNOLOGY 3, 133–151 (1992)

Performance Optimization of a High-Repetition-Rate KrF Laser Plasma X-Ray Source for Microlithography

FRED BIJKERK, ERIC LOUIS, MARNIX J. VAN DER WIEL, EDMOND C. I. TURCU,* GREG J. TALLENTS,*,[1] AND DIMITRI BATANI[2]

*FOM-Institute for Plasma Physics Rijnhuizen, Edisonbaan 14, 3439 MN Nieuwegein, The Netherlands; and *SERC Rutherford Appleton Laboratory, Chilton Didcot, Oxon OX11 0QX, United Kingdom*

Received July 22, 1991; revised February 3, 1992

In order to develop a high-intensity laser plasma x-ray source appropriate for industrial application of x-ray lithography, experiments have been carried out using a high-repetition-rate (up to 40 Hz) excimer laser (249 nm, 300 mJ) with a power density of 2×10^{13} W/cm^2 in the laser focus. In this study emphasis is given to remedying specific problems inherent in operating the laser plasma x-ray source at high repetition rates and in its prolonged operation. Two different methods of minimizing the production of target debris are investigated. First, the use of helium as a quenching gas results in a reduction of the amount of atomic debris particles by more than two orders of magnitude with negligible x-ray absorption. Second, a tape target as opposed to a solid target reduces the production of larger debris particles by a further factor of 100. Remaining debris is stopped by an aluminized plastic or beryllium filter used to avoid exposure of the resist by plasma ultraviolet radiation. The x-ray source has been used to image x-ray transmission mask structures down to 0.3 μm onto general purpose x-ray photo-resist. Results have been analyzed with SEM. The x-ray emission spectrum of the repetitive laser plasmas created from an iron target has been recorded and the conversion efficiency of the laser light into x-rays that contribute to exposure of the resist was measured to be 0.3% over 2π sr.

I. INTRODUCTION

X-ray microlithography, the imaging method for integrated circuit pattern replication using x-ray radiation, is generally considered to have advantages over optical lithography. Most notable are better resolution, a simpler chemical process, and insensitivity to dust.

For industrial IC manufacture, the need for compact x-ray sources capable of delivering high average x-ray power is now well established (*1, 2*). Candidate sources are (i) dedicated electron-storage rings, (ii) plasma-focus devices, and (iii) laser plasmas. Dedicated electron-storage rings are presently in the process of being commissioned and will be able to serve many beamlines for the large-scale manufacture of IC devices. Parallel development of the latter two source types is being pursued as they are expected to be suitable for small-scale applications, hence requiring less clean-room space and

[1] Permanent address: Department of Physics, University of Essex, Wivenhoe Park, Colchester CO4 35Q, United Kingdom.

[2] On leave from Instituto di Fisica Atomica e Moleculare, CNF, Pisa, Italy.

0895-3996/92 $5.00

less capital investment. Compact and economical sources should enable industrial application of x-ray lithography at a favorable performance-to-cost ratio.

The potential of laser plasma x-ray sources is becoming increasingly evident, largely due to the rapid development of efficient lasers, such as excimer gas lasers and slab-geometry glass lasers. Proofs of principle, in which laser plasma x-ray sources were used to replicate submicrometer patterns, have already been obtained (*3–8*). However, virtually none of these systems have been demonstrated to operate at the degree of sophistication required for industrial semiconductor device manufacturing. Of particular importance in order to guarantee a defect-free pattern replication is the need to eliminate debris expanding from the laser plasma. Demonstration of this industrial level of operation should speed up the switchover from present-day optical lithography to x-ray lithography.

This paper describes development steps in the optimization process of the laser plasma x-ray source. It is a scaling study toward operation of this type of x-ray source at high repetition rates and addresses problems such as the achievement of high average x-ray intensities and contamination of plasma facing surfaces by target debris from the plasma.

We report the first laser plasma x-ray microlithography experiments carried out at repetition rates up to 40 Hz and the first x-ray lithography exposures at He pressure of 1 bar. It is demonstrated that sub-0.5-μm structures can be faithfully reproduced into a general purpose x-ray photo-resist now considered a standard material in synchrotron microlithography (*9*).

Ideas for further upgrading this type of x-ray source in the near future are presented. Incorporating these upgrades, of which some have already been successfully tested (*10, 11*), will mean that a full resist exposure time within 10 s can be realistically anticipated. Practical device manufacturing is then possible using compact, high-brightness laser plasma sources with x-ray intensities comparable to those from conventional electron-storage rings (*12*).

II. EXPERIMENTAL ARRANGEMENTS

The experimental work was carried out with the laser plasma x-ray source located at the Laser Support Facility of the Rutherford Appleton Laboratory (*5*) (Fig. 1). The source is generated by a system consisting of two commercial KrF lasers (Questec 2440) which in the present configuration yield a total pulse energy of 300 mJ at repetition rates up to 100 Hz. The lasing wavelength λ is 249 nm and the pulse duration is 18 ns. The laser system is operated with an injection-locked unstable resonator amplifier. A low beam divergence is achieved, measured in the equivalent focal plane of a 5-m focal length lens to be 100 μrad ($1/e$). The low beam divergence enables tight focusing so that a sufficiently hot plasma can be created with moderate pulse energy. With a 90-mm aspheric singlet lens the resulting focal diameter is 10 μm and the power density is 2×10^{13} W/cm^2.

It is noted that this application of excimer lasers does not require special line-narrowing techniques such as have been found necessary for excimer deep-UV lithography (*13*). The injection-locking technique employed here does not impose any practical difficulties in operation.

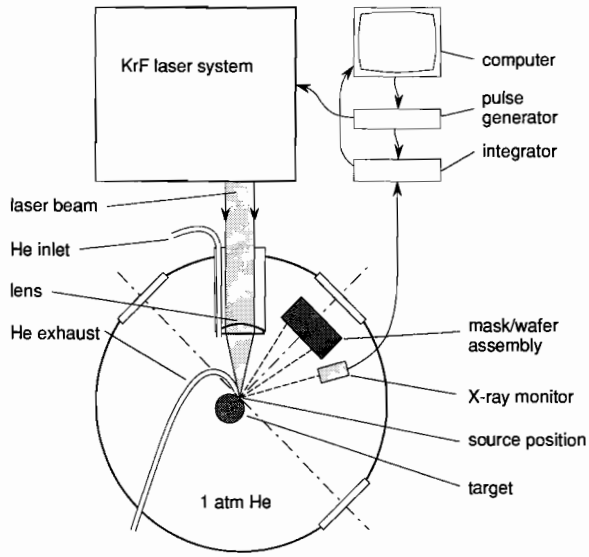

FIG. 1. Outline of the experimental arrangement.

The repetitive plasmas are normally created on a solid Fe rod which simultaneously rotates and translates to ensure that each pulse is focused on fresh target material. Some results are presented where the target is a 60-μm-thick Fe tape (Section IIIE). The laser energy is focused onto the target so that the normal is at 45° to the laser beam axis. To limit target debris from the plasma, He is flowed into the source chamber at atmospheric pressure. The source can also be operated under vacuum.

All measurements in this study have been performed using a He flow rate of at least 10 liter/min at a pressure of 1 bar. The He flows from a distribution ring around the lens to an outlet close to the position of the plasma. The He flows counter to the direction of the expanding plasma and debris in order to protect the lens surface. The flow is found to be essential for stable operation of the source if He is used. In static He, a particle cloud is created which partly absorbs the UV laser light, resulting in a diminished x-ray yield.

X-ray emission spectra of the plasma are recorded on photographic film (Kodak DEF) using a flat crystal spectrometer (KAP crystal, $2d = 2.663$ nm) (*14*). The spectrum recorded by the spectrometer, with a resolution ($\lambda/\Delta\lambda \approx 500$) limited by the plasma source size, is filtered with 18-μm-thick Be to stop UV and visible light from exposing the film. The spectrum on the film is converted to an intensity scale using tabulated calibration data (*15*) and a computerized densitometer.

An analysis of target-debris production is undertaken by arranging for fused silica plates to be coated by the debris from the repetitive plasmas. The absorption of the coated debris layer at optical wavelengths ($\lambda = 440$ and 540 nm) is measured using a dual-beam differential spectrophotometer. The thickness of the coated material is determined from this absorption using tabulated absorption coefficients (*16*). Optical microscopy at magnification of $\sim$500 is used to investigate the sizes of macroclusters

emitted by the plasma and to determine the areal density of holes produced by these clusters in thin filters.

A special wafer holder is used for the actual exposure of photo-resist. It contains the x-ray mask and the resist-coated wafer and can be placed at various positions in the source chamber. The masks employed are copies of TESMA masks (test absorber geometries) and masks with other pattern geometries supplied by the Fraunhofer Institut für Mikrostrukturtechnik (Berlin, FRG). They consist of a 2.1-μm Si membrane with 1-μm Au absorber patterns with feature sizes down to 0.3 μm. The x-ray mask and the wafer are separated by a 25-μm proximity foil. We use standard formula Ray-PF photo-resist, spin-coated onto 3-in. Si wafers to a thickness of 1.2 μm, and prebaked at 110°C for 60 s. After exposure and 15 min holding time, the resist is developed in 1 + 1 diluted AZ developer for 120 s. Subsequently the wafers are postbaked at 80°C for 25 min. The resist structures are inspected by SEM microscopy after Au sputter coating and the resist layer thickness is determined by mechanical stylus measurements.

Accurate control of the x-ray dose delivered to the photo-resist is obtained by an x-ray monitor. The monitor consists of an absolutely calibrated semiconductor diode at a fixed position in the source chamber and an ADC signal integrator. The successive signals from the monitor are accumulated by a computer, which stops the laser system as the preset x-ray dose is attained. In our experiments identical filters are used for the monitor and the photo-resist to exclude uncertainties in dose due to filter characteristics. An additional diode is used to measure the x-ray emission of the plasma at different positions in the source chamber. The signal of the x-ray diode is displayed on a 350-MHz oscilloscope simultaneously with the signal of a fast UV diode monitoring the laser pulses.

III. RESULTS AND DISCUSSION

We assess the characteristics of the high-repetition-rate x-ray source and its optimization for microlithography. For most of the problems encountered experimental investigations of possible solutions have been undertaken.

A. X-Ray Spectrum

An x-ray spectrum of the laser plasma emission used to expose the photo-resists is obtained using a flat KAP crystal spectrometer with recording on Kodak DEF film (Fig. 2). A solid Fe target[3] such as that used for the exposures of the masked resists is used. For full exposure of the film in the Be-filtered spectrometer, 210 laser plasma pulses were accumulated. The spectrum is converted to an absolute intensity scale using the calibration (*15*) of the Kodak DEF film and corrected for (i) varying crystal reflectivity (assuming a perfect crystal) (*17*) and (ii) the wavelength-dependent attenuation of an 18-μm-thick Be foil used in the spectrometer to prevent visible light from exposing the film. We have used the wavelength integrated signals recorded by a Si p-i-n diode exposed directly to the x-ray emission to calibrate the integrated reflectivity of the KAP crystal.

The calculated average photon wavelength emitted is approximately 1.4 nm (0.9

[3] Chemical composition: Fe (>97.5%), C (1%), Si (<0.5%), Cr (<0.5%), and Mn (<0.5%).

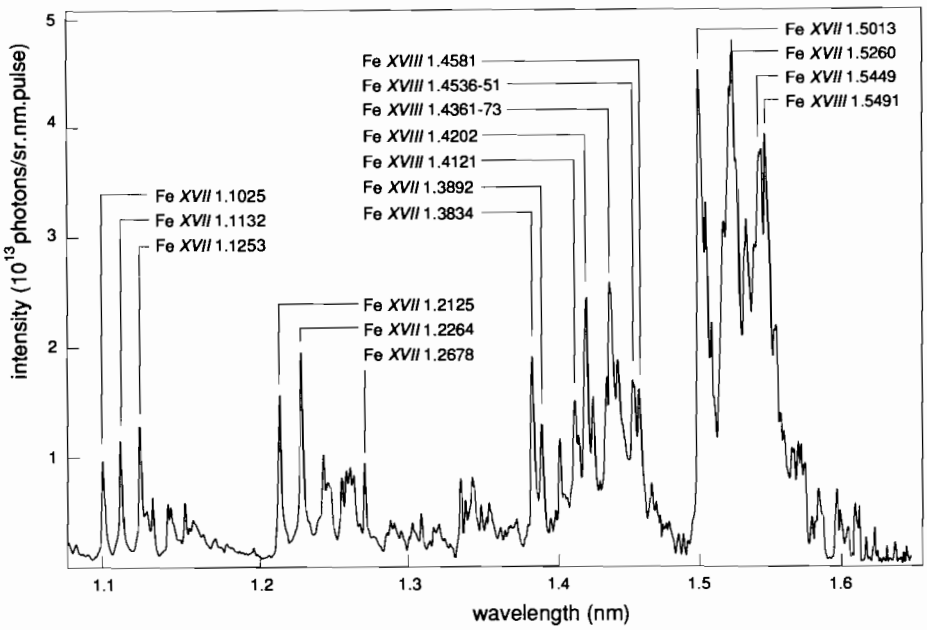

FIG. 2. The emitted Fe spectrum allowing for film calibration, spectrograph crystal reflectivity, and filter transmission.

keV), but there are spectral lines with significant intensity over the entire range 1.1 to 1.6 nm. The more intense spectral lines originate from electronic bound–bound transitions in multicharged ions, namely M- to L-shell transitions (principal quantum number n = 3–2) of Ne-like (Fe XVII) and F-like (Fe XVIII) ions (*18–20*). The irradiance on target amounted to 2×10^{13} W/cm^2, necessary for efficient generation of short-wavelength ($\lambda < 2$ nm) x-ray emission from laser plasmas (*21, 22*).

The wavelength band of interest in x-ray lithography is determined by numerous factors such as mask transmission, Fresnel diffraction over the mask–wafer gap, resist absorption, and secondary radiation in the resist. In general it ranges from ~1.7 to ~0.7 nm. The exposure efficiency $\eta(\lambda)$ of the transmission x-ray lithographic process can be characterized by the product

$$\eta(\lambda) = \tau_f(\lambda)\tau_m(\lambda)\alpha_r(\lambda), \qquad [1]$$

in which $\tau_f(\lambda)$ is the transmission of a protective foil/UV filter placed in front of the x-ray mask, $\tau_m(\lambda)$ is the transmission of the mask membrane, and $\alpha_r(\lambda)$ is the absorption in the photo-resist. This product is shown in Fig. 3i as a function of wavelength λ for the filter and resist materials used in this study (see Table 1). Curve a shows $\eta(\lambda)$ for a protective foil consisting of aluminized plastic (A in Table 1), whereas for curve b a 6.2-μm Be protective foil is used (B in Table 1). In both curves transmission of a Si mask membrane and a Au film (deposited on the mask membrane for production of the absorber structures) is included. The transmission products $\tau_f(\lambda)$ $\tau_m(\lambda)$ through

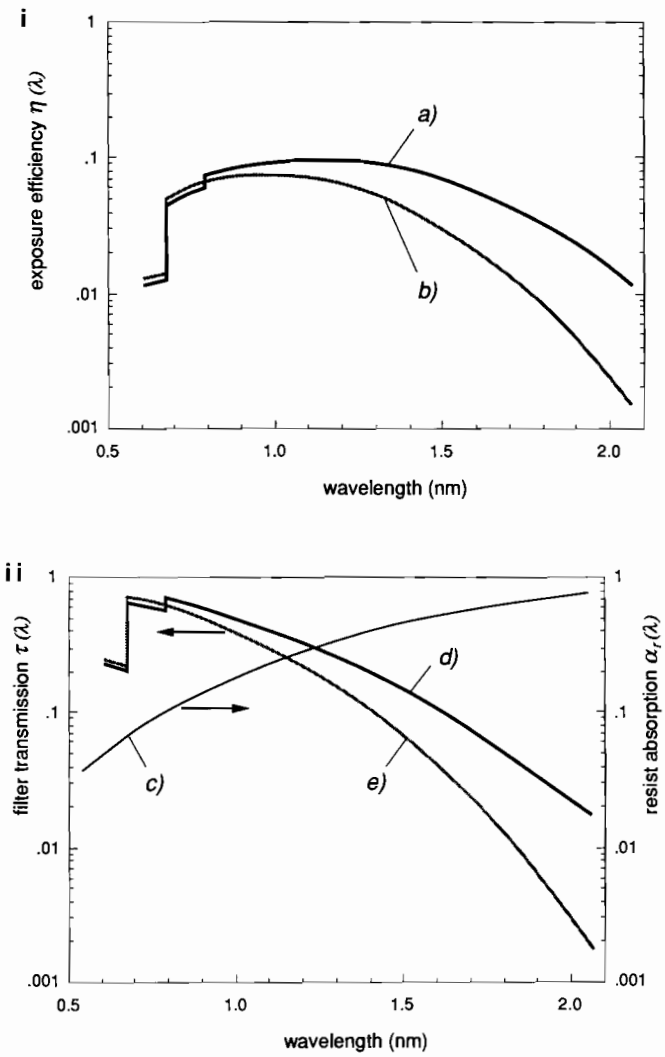

FIG. 3. (i) Exposure efficiency $\eta(\lambda)$ of the transmission x-ray lithographic process plotted as a function of wavelength λ for the filter and resist materials used in this study. Curve a shows $\eta(\lambda)$ for filter set A, curve b for set B (see Table 1) with Ray-PF resist of 1.2 μm. (ii) Absorption $\alpha_r(\lambda)$ in 1.2-μm Ray-PF resist (curve c) and transmission $\tau_f(\lambda)$ $\tau_m(\lambda)$ for filter/mask combination set A (curve d) and for set B (curve e).

these two filter/mask combinations (sets A and B) are separately plotted in Fig. 3ii, as curves d and e. The absorption $\alpha_r(\lambda)$ of a 1.2-μm-thick layer of Ray-PF resist (*23*) is also shown (curve c).

The exposure efficiency $\eta(\lambda)$ with filter set A (curve a) is nearly constant over the spectral range 0.9 nm $< \lambda <$ 1.6 nm, which is the range of intense emission of the Fe plasmas. Soft x-rays are absorbed more in the filter and mask, but are simultaneously more efficient in exposing photo-resist. Clearly a high exposure efficiency $\eta(\lambda)$ can be achieved for wavelengths up to 1.7 nm if highly transparent filters like set A can be

TABLE I

Composition of Filters/Mask Membrane

Set	Composition
A	0.2 μm Al + 0.4 μm $(CH_2{=}CHCH_3)_n$ + 2.0 μm Si + 25 nm Au
B	6.2 μm Be + 2.0 μm Si + 25 nm Au

used. Operation of a source at relatively long wavelengths has the advantage of an efficient utilization of radiation due to the high absorption in the photo-resist (40% at 1.4 nm). The use of thin filters is suitable only if there is a sufficiently small production of target debris (see following sections).

A second consideration for using relatively long-wavelength radiation is connected more specifically to the laser plasma. In general for this type of x-ray source, high laser light conversion into x-rays can be achieved with wavelengths down to $\sim$1.2 nm (*21*). The conversion into shorter wavelength radiation is generally lower. Our choice for Fe as a laser target is based on this. In a separate experiment we compared the conversion of Fe x-ray radiation, peaked at $\lambda \approx 1.4$ nm, with the conversion into Cu x-ray radiation, mainly emitting at $\lambda \approx 1.0$ nm. A significantly lower (1/3) conversion efficiency is found for Cu plasmas, although generated with the same target irradiance. The use of long-wavelength radiation results in good contrast in the resist image, even when only thin layers of mask absorber structures are used. This facilitates x-ray mask fabrication.

In the case of lithographic 1:1 imaging with a finite proximity distance between mask and wafer, Fresnel diffraction imposes a upper limit on the wavelength usable for imaging. The diffraction-limited resolution δ is given by $\delta = 0.8\sqrt{\lambda g}$, in which g is the proximity distance. As an example, a resolution of 0.10 μm is feasible with an x-ray wavelength of $\lambda \approx 1.4$ nm (as in this study) and an $\sim$10 μm proximity distance (*24, 25*). Much longer wavelengths are therefore less suitable.

B. Geometry of Exposure

We have measured the angular distribution of the plasma's x-ray emission in order to determine the proper angle relative to the target for the lithographic exposures to be carried out (Fig. 4). The x-ray intensity shows a maximum at the target normal, which is at 45° to the laser beam axis. In previous experiments, where the laser beam was focused at normal incidence on the target, the x-ray intensity was similarly peaked in the direction of the target normal. Hitting the target at 45° incidence to the normal is a clear advantage for lithographic experiments, since the exposure can benefit from the maximum x-ray intensity along the target normal.

The measurements shown in Fig. 4 are made for the two sets of diode filters given in Table 1. The two sets correspond to different energy ranges of the spectrum: filter set A is primarily transparent to low x-ray energies, as opposed to set B. The difference in angular distribution observed in Fig. 4 is, therefore, explained in terms of an energy dependence of the distribution, most likely related to the expansion mechanism of the plasma. The high-temperature plasma core radiates higher energy x-rays spherically,

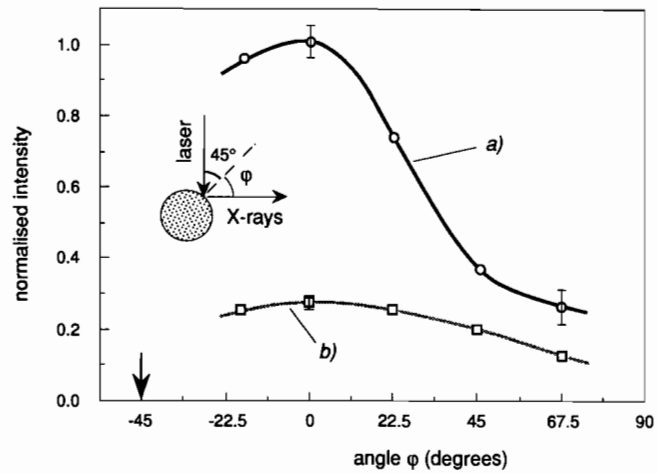

FIG. 4. Angular distribution of x-ray emission. Curve a is recorded with filter set A and curve b with set B. For both curves the maximum is along the target normal. The inset shows the geometry of laser beam and x-rays.

whereas the plasma plume of lower temperature radiates lower energy x-rays preferentially in the forward direction. This is probably caused by greater self-absorption of the soft x-rays emitted in directions away from the target normal where the plasma is thicker and Doppler decoupling is less important (*26*).

The angular distribution given in Fig. 4 allows us to determine the homogeneity of the illumination of photo-resist. Small differences in exposure dose, e.g., between the center and the edge of the exposure field, may give rise to reduced linewidth control. To avoid this, illumination should be uniform to within ~10%. Although curve a follows a sharp $\cos^{(4\pm1)}\phi$ behavior, a uniformity of better than ±2.5% can be obtained over a 20×20 mm^2 exposure field at a source-to-mask distance of 100 mm. In the case of curve b, which follows a $\cos\phi$ behavior, the uniformity is better than ±0.5%. Both uniformity values are sufficient for IC-production circumstances and the use of high-gradation photo-resists.

C. Absolute Conversion Efficiency

Given the relative x-ray spectral distribution in Fig. 2, the absolute intensity of the x-ray source can be calculated from the signals of the x-ray diode. We use the sensitivity-versus-wavelength data supplied by the diode manufacturer (*27*), taking into account the transmission of the diode filters. As a result we obtain a conversion efficiency of laser light into Fe x-ray emission (1.1 to 1.6 nm) of 0.11% sr^{-1}. This value is obtained using a diode at 0° to the target normal. Combining this result with the angular distribution of the x-ray intensity given in the previous section, we obtain a total conversion efficiency over 2π sr of 0.28%. Expressed in terms of x-ray energy at the surface of the photo-resist placed along the target normal at 100 mm from the source, this corresponds to a value of 0.85 μJ/cm^2 per pulse. For these measurements filter set A is used (Table 1). Since the diode and the photo-resist are filtered with identical

filters, this value for the x-ray energy at the resist is not influenced by errors in filter transmission.

The conversion efficiency is lower than values reported in the literature by at least one order of magnitude. A major difference between the present experiment and the experimental conditions quoted in the literature is the fact that our spotsize of 10 μm is a factor of 10 smaller (*21*). The small focus is needed to obtain a sufficiently high power density with the available laser energy and laser pulse duration. Lateral transport of energy out of the small focal region may be greater in our experiment. A plume of low-density plasma could also stop the penetration of laser energy to the x-ray emitting region of the plasma. In a separate time-resolved experiment, using a subnanosecond response diode, a drop in $\sim$1.4-nm x-ray emission can be observed long before the laser pulse ends. This could indicate such a stoppage of laser energy absorption. Nevertheless the peak conversion efficiency from KrF lasers is in good agreement with data from the literature. Two approaches might solve the problem. First, the spotsize could be increased, while keeping the irradiance constant. This requires a higher laser energy, probably of the order of one to several Joules per pulse. Second, the pulse duration could be reduced. This approach has been investigated elsewhere (*10*). A significant enhancement of the conversion efficiency up to 2.4% using similar irradiance and target material was obtained when an excimer laser was injection mode-locked to generate a pulse train of 150-ps pulses.

D. Atomic Debris

An unwanted side effect of laser plasma x-ray emission is the production of debris from the laser target. Target debris, varying from atomic sizes up to clusters of $\sim$1 μm, can be deposited on optics and x-ray filters. Large clusters can penetrate protective filters and damage the masks or produce shadowing effects in the resist (see Section IIIE). Debris production can be considerable, especially if a large number of pulses are required. By measuring the volume of the crater in the target the amount of evaporated material can be calculated. We find a total of $\sim$7 μg of Fe evaporated over 2π sr per pulse. It is obvious that this problem should be eliminated if the source is to be used for industrial applications.

All our lithography exposures so far have been undertaken with helium gas of atmospheric pressure in the source chamber. This has proved to be an extremely effective method of reducing target debris (*11, 28*). To illustrate the effect quantitatively, we measured the deposition rate of atomic-scale target debris onto quartz plates under vacuum and in 1 bar He (Fig. 5). The plates were placed at 77 mm from the target at different angles ϕ and exposed to target debris in a series of 1.5×10^4 and 4×10^4 laser pulses on the Fe target. The thickness of the debris layer $z(\phi)$ is determined from the visible light transmission $T(\lambda)$ through the quartz plates, using tabulated values for the light extinction coefficient $k(\lambda)$ (*16, 29*). The coated debris thickness is given by

$$z(\phi) = \frac{\lambda \ln T(\lambda)}{-4\pi k(\lambda)}. \qquad [2]$$

For Fig. 5, the measured layer thickness $z(\phi)$ is converted to the deposition rate $\eta(\phi)$ expressed in nanograms per steradian per pulse. The results from measurements

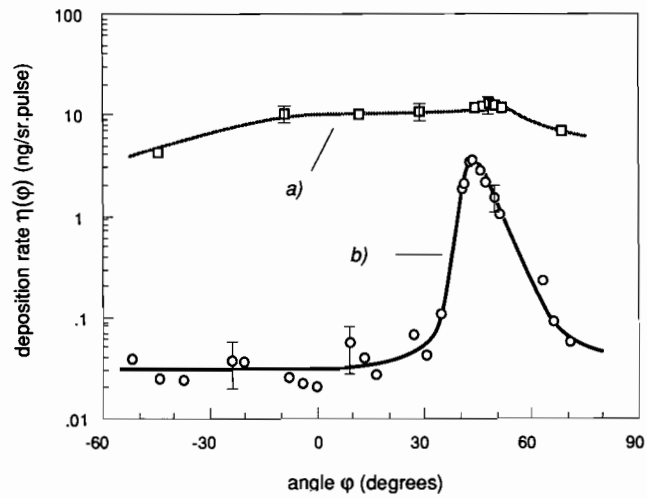

FIG. 5. Deposition rate $\eta(\phi)$ of target debris as a function of angle ϕ to the target normal (a) under vacuum conditions, (b) in He at atmospheric pressure.

with different numbers of laser pulses are found to be reproducible to within ±10%. The laser energy remained stable typically to ±5% for any measurement. We estimate an overall absolute error in the deposition rate measurements of below 40%.

From Fig. 5 it is obvious that applying He buffer gas results in a drastically reduced debris deposition rate for all angles except around 45°. The reduction amounts to at least a factor of 10^2 and can therefore be considered as effective. For a single typical lithographic exposure the remaining deposition is ~0.1 nm of debris, which can be stopped simply by a protective filter. This filter could be made as a movable tape to allow continuous operation of the source.

The effectiveness of He buffer gas in quenching debris can be explained qualitatively by assuming momentum transfer of Fe vapor to He atoms. Although the Fe to He mass ratio is high (56:4), the He density at atmospheric pressure is sufficient to produce the observed effect (*30*). We can expect a mean free path of ~2.5 μm, using a scattering cross section of 10^{-20} m^2. Debris can be thermalized to ambient temperature within less than 100 μm from the plasma.

Figure 5 shows that the deposition rate in He is nearly constant over a wide range of angles ϕ, apart from the strongly enhanced deposition at $\phi = 45°$. Such an isotropic polar distribution supports the momentum transfer mechanism, since multiple Fe–He collisions will lead to random directions of the thermalized Fe vapor. The observed effect is likely to be proportional to at least the inverse third power of distance, due to the inverse square radial decay multiplied by the debris trajectory. At distances larger than the 77 mm used for this measurement the reduction in deposition will be more pronounced.

The enhanced deposition rate at $\phi = 45°$ might be caused by shock wave reflection in the solid target. Alternatively, in He atmosphere the flow of He may affect the trajectory of the debris, while for vacuum conditions the similar although much smaller

peak of debris observed may be due to the presence of a Fe particle cloud close to the target surface, causing an effect similar to that of the He atmosphere (Fig. 5).

The reduced deposition rate when He gas is used in the source chamber results in a reduction in coating of the focussing lens by plasma debris. The transmission of the lens for the KrF wavelength of $\lambda = 249$ nm was monitored using a spectrophotometer. Under vacuum conditions the transmission was reduced by 39% after 1.9×10^4 laser pulses, whereas under operation at atmospheric pressure of He the transmission was reduced by 24% after 3.8×10^5 laser pulses. In practice the lens required cleaning every 10^7 laser pulses. The observed reduction in coating is less than that determined from the measurements with the plates used for Fig. 5. The lens transmission appears to benefit from a self-cleaning effect of the laser beam. The central region where the laser beam passes through remains significantly cleaner than the surrounding region. The numbers given for transmission correspond to this clean region.

Application of He in the source chamber is possible because the absorption of x-ray radiation in He is low for wavelengths below 1.5 nm. This is demonstrated by measuring the integrated x-ray intensity with the x-ray diode at 240 mm from the source in atmospheric He. Compared to vacuum conditions the diode signal dropped to $76 \pm 5\%$, which is in agreement with the calculated He transmission of 72% (*31*). Given the 5% accuracy of this measurement, it also implies that the x-ray yield of the plasmas is not affected, which indicates that negligible laser energy is absorbed in the helium. The breakdown threshold of He for KrF laser radiation at $\sim 10^{13}$ W/cm^2 is $\sim$400 Torr (*32, 33*). However, the laser energy absorbed in the breakdown by operating just above threshold is less than 10%.

It can be calculated that the x-ray intensity at the surface of the photo-resist at 100 mm distance from the target after passing through 1 bar He amounts to 87% of the emitted x-ray intensity. This small loss in intensity is certainly tolerable in view of the drastically diminished debris deposition.

Operation of a source with He flowing at atmospheric pressure is particularly useful for cooling the x-ray masks. The thin mask membranes are easily subjected to distortions due to heat-induced stress. A slow flow of He can overcome this. Additionally, frequent loading of wafers is prohibitively complex under vacuum exposure conditions and is facilitated in an environment at atmospheric pressure.

We have investigated the maximum repetition rate at which the source can be operated while maintaining a constant x-ray yield per pulse. In our test the repetition rate is limited by the He flow rate, which stops the buildup of a particle cloud from debris. For practical reasons the flow rate is limited to 40 liter/min, allowing operation of the source at up to 40 Hz. The required flow rate appears to scale linearly with the repetition rate and we expect no physical limitation to scaling up to higher repetition rates. With ultrathin tape carbon laser targets, giving less debris per pulse, operation at a repetition rate of 100 Hz can be realized without reduction of the x-ray yield (*34*).

E. Cluster Debris

In addition to the debris of atomic size considered so far, damage by micrometer-sized debris or "cluster debris" is studied also. Due to their very high momentum, high-speed clusters are very destructive, especially for delicate filters and x-ray masks.

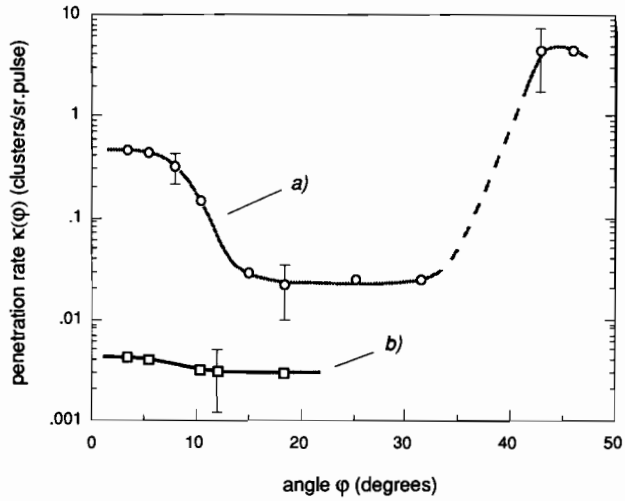

FIG. 6. Areal penetration rate $\kappa(\phi)$ of cluster-like debris as a function of angle ϕ. $\kappa(\phi)$ is the number of clusters per steradian per pulse penetrated through protective filters at 100 mm. (a) Solid Fe rod laser target, (b) 60-μm Fe tape laser target.

In order to analyze contamination by this type of debris, a second method is used to quantify penetrating clusters. The method is based on the consideration that any lithographic exposure setup will include some filter of minimal thickness in order to stop the UV and visible radiation from the plasma. Accordingly we selected an appropriate filter and investigated the areal penetration by debris clusters after exposure to the repetitive plasmas. For many years, polypropylene filters have proven to be very successful due to their strength and high transmission in a broad wavelength range. The filter characteristics necessary for this application are achieved by coating the 0.4-μm-thick polypropylene with 0.2 μm Al. The total filter possesses a transmission of 82% at 1.4 nm. These filters are exposed to cluster debris in a series of 2×10^4 to 7×10^4 laser pulses. Afterward the areal density of penetrated clusters is determined by investigating the number of holes in the filters with optical microscopy. Since the holes are in general larger than the clusters producing them the method also records small (<0.5 μm) clusters with sufficient momentum to penetrate the foils. The result of the measurement is given in Fig. 6 (curve a), where the areal penetration rate $\kappa(\phi)$ is shown as the number of penetrated clusters per steradian per pulse at 100 mm from the plasmas.

The data of curve a were obtained using a laser target consisting of a solid Fe rod. To further suppress debris we replaced the rod by a thin target consisting of a 60-μm-thick Fe tape. The measurement using this tape target resulted in curve b.

A comparison of the two curves of Fig. 6 shows the remedying effect of thin tape targets to be quite obvious. For small angles ($\phi \leq 15°$) the reduction in areal penetration amounts to two orders of magnitude. In addition to applying buffer gas against atomic debris, use of a thin tape target is therefore considered a most effective remedy against cluster debris. A possible loss in x-ray production, determined in a preliminary ex-

periment to be within 10%, is acceptable. A reduction in atomic debris also occurs using the tape targets.

The penetration rate with tape targets is diminished because less material can be evaporated and a substantial part of the material can be ejected at the rearside of the tape. The laser pulse produces craters in solid targets with a typical depth of ~75 μm.[4] The 60-μm-thick tape targets are therefore penetrated so that most of the debris is ejected backward, pushed by a plasma-produced shock wave. X-ray production is only marginally affected, because the sub-2-nm x-ray radiation is only generated in a thin (several micrometers) plasma layer. The cluster debris is mainly produced from deeper target material.

F. Resist Characterization and Replication of Structures

Knowing the characteristics of our source, we have exposed x-ray photo-resist to characterize its sensitivity, resolution, and gradation. A general purpose x-ray resist (Ray-PF) which is used as a standard material for synchrotron exposures was selected. Ray-PF is a novolak-based three-component system of positive tone. The concept of three-component systems makes high sensitivities possible while maintaining stability of the resist material under the process steps that follow lithography. An optimized version of this resist was sufficiently sensitive to be patterned with x-ray radiation generated by a single laser pulse (*35*). For all source types, sensitivity of applied resists is paramount since it directly correlates to wafer throughput and hence to cost effectiveness of the lithographic exposure.

The measured gradation curve of the resist is shown in Fig. 7. The figure shows the normalized remaining resist film thickness (RFT) as a function of the exposure doses in the case of over-, nominal-, and underdevelopment (resp. curves a, b, and c). The resist is exposed to a range of controlled x-ray doses and developed in diluted AZ developer. The RFTs are then measured by a mechanical stylus. Under nominal development conditions and an initial layer thickness of 1.2 μm, the resist exhibits a sensitivity of 18 mJ/cm^2. This sensitivity is higher than values obtained from exposures by synchrotron radiation at BESSY (Berlin, FRG), where a sensitivity of ~50 mJ/cm^2 was measured for Ray-PF. The higher sensitivity obtained from our measurements is explained by the more efficient absorption of the longer wavelengths used here. For measurement of the gradation curve filter set A is used.

The gradation γ shown in Fig. 7 is approximately 11 and is not measurably dependent on development time. Similar values have been obtained from exposures with synchrotron radiation (*9*). Our observation that the gradation does not measurably vary under different development conditions suggests a certain process latitude.[5] However, the actual process latitude can only be quantified by taking into account variation of linewidths of the replicated structures.

The observed gradation is in the upper range of known resist materials, which is advantageous for achieving high resolutions. As an example Fig. 8 shows scanning

[4] A small part of this is coated onto our substrates (~5%); the remaining part is probably trapped by the nearby inlet to the vacuum pump.

[5] Process latitude: the tolerance in exposure dose that can be allowed for a certain resist linewidth variation.

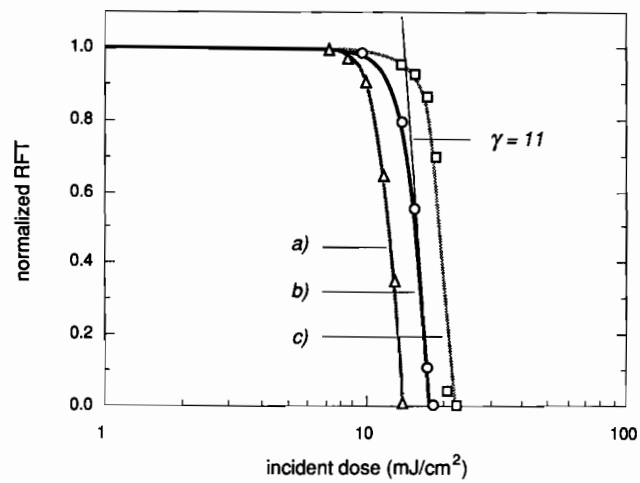

FIG. 7. Photo-resist gradation curve determined by exposure from the laser plasma. Full-depth exposure at nominal development time (curve b) requires 18 mJ/cm^2. Curves a and c represent resp. overdevelopment (+25%) and underdevelopment (−40%).

electron micrographs of 0.3- and 0.5-μm structures printed in a 1.2-μm-thick layer of resist. The resist structures exhibit the steep sidewalls characteristic of x-ray exposures. The resist pattern replicates the imaged mask absorber pattern within an estimated accuracy of 50 nm. Figure 7 represents patterns replicated from the smallest structures on the masks, indicating that the resolution limit of the combination of source and resist is better than our measured 0.3 μm. Further research using masks with smaller features is therefore desirable to determine the limit in achievable resolution. The nominal development conditions of the resist are used. The exposures are not performed under clean-room conditions, which demonstrates the insensitivity of the process to low-atomic-number particulate defects.

For a full-depth exposure of the masked resist a preset dose of 20 mJ/cm^2 was supplied to the resist. The source was operated at 20 Hz, which yields an average x-ray power density at the surface of the resist of 4.8 $\pm$ 0.4 μW/cm^2. For these exposures filter set B was employed in the monitor diode. Under these conditions a full exposure requires 67 min. The dose required for exposure using set B is slightly higher than the dose using set A, which is also used to determine the gradation curve. As can be seen from Fig. 3ii (curve d), set A is more transparent for softer radiation which is more efficiently absorbed in the resist. For filter set A the x-ray power density at the resist amounts to 17.0 $\pm$ 1.5 μW/cm^2, yielding a full exposure time of 18 min.

All exposures are carried out at a source-to-mask distance of 100 mm and at an angle ϕ between 15° and 30° relative to the target normal. The choice for the angles is dictated by the debris characteristics and the angular distribution of x-ray emission. First, angles $\phi > 30°$ are excluded due to the high deposition rate at angles around

FIG. 8. Scanning electron micrographs of photo-resist exposed through Si-based x-ray masks. Thickness of resist layer is 1.2 μm. (a) 0.5- and 0.6-μm patterns, (b) 0.3-μm spaces.

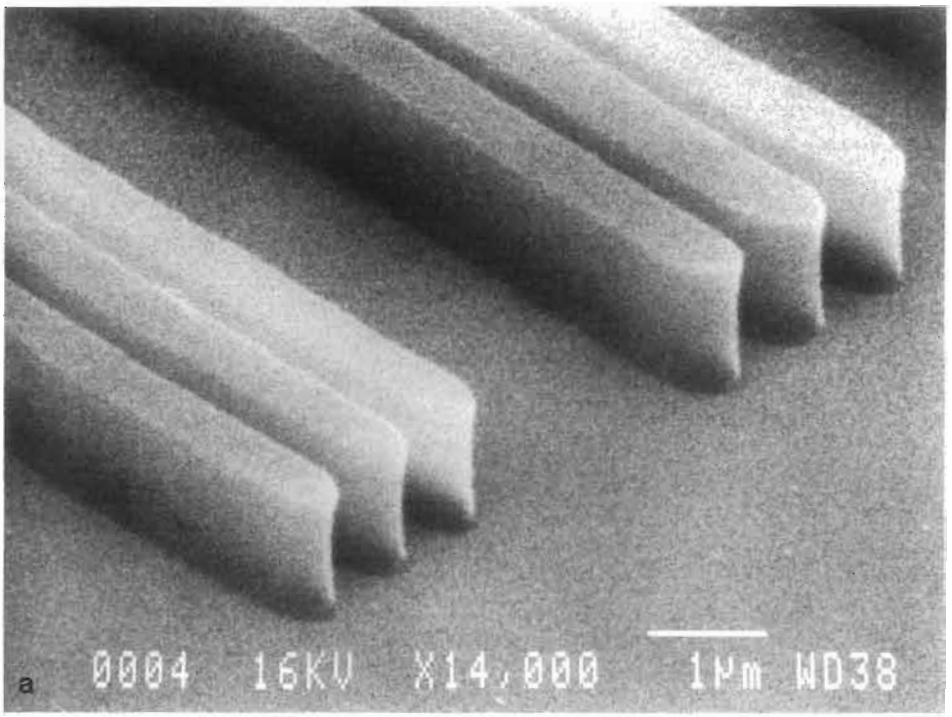
a
0004 16KV X14,000 1μm WD38

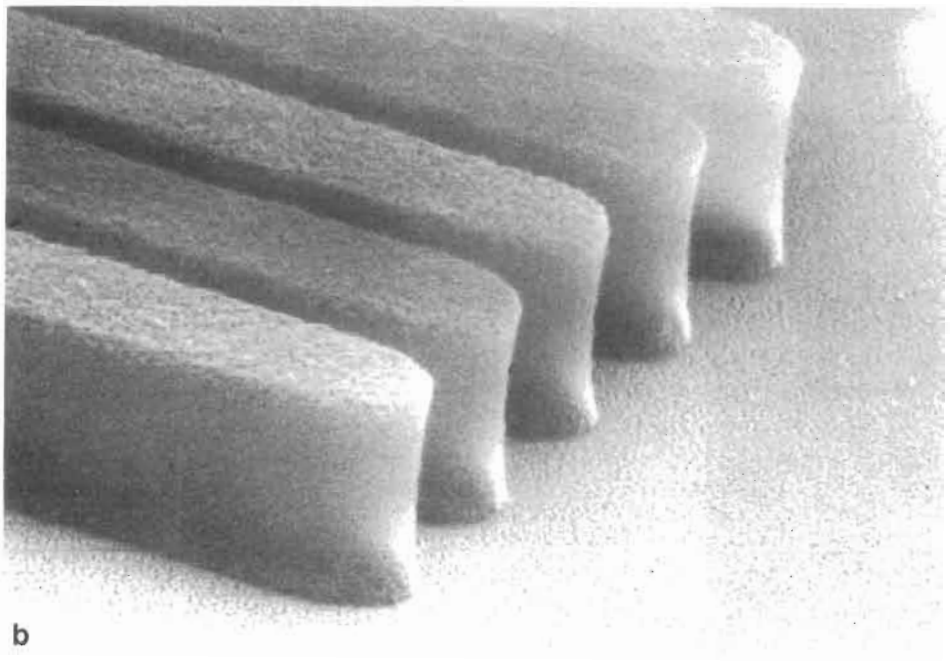
b

45° (Section IIID); second, angles $\phi < 15°$ are prohibited due to the high density of penetrating clusters in that region (Section IIIE). For exposure of masked resist we use the solid Fe target. We reiterate that the limitation to angles $\phi > 15°$ can be eliminated if tape target is used. It would then be possible to benefit from the maximum x-ray yield along the target normal, as well as the slower angular variation of x-ray intensity around the target normal.

The achievable resist resolution is not limited by the size of the x-ray source. The source size, as previously determined from x-ray pinhole camera pictures (*11*), amounts to <20 μm. The resulting penumbral blur of <5 nm is negligible compared to other imaging faults from, e.g., x-ray beam divergence or mask instabilities.

IV. FUTURE DEVELOPMENTS

The present work allows assessment of a number of factors which should lead to a considerably higher x-ray power density and hence to a shorter exposure duration (Table 2). This can be realized with the present laser system. A factor of 10 can be achieved by increasing the laser repetition rate from 20 to 200 Hz. This will require an enhanced flow of He to flush the metal cloud from the vicinity of the target. Another factor of 10 can be gained in the conversion efficiency if the present laser is injection mode-locked to generate a train of short pulses (~100 ps) rather than a single nanosecond pulse. (Enhancing the pulse energy to ~1 J is expected to give a similar improvement.)

An enhancement of 2–4 can be obtained by using an aluminized plastic filter (with transmission of ~90%) as opposed to a Be filter. This will be possible if the target consists of a thin tape as discussed in Section IIIE. The overall possible x-ray enhancement feasible with these modifications to our present laser system should be ~200–400 which will permit exposure times of ~10 s for full-field resist replication of masks. This corresponds to an intensity of ~2 mW/cm^2 at the resist, which is sufficient for

TABLE 2

Summary of Problem Areas and Investigated Remedies

(a) This work

Problem	Main remedy	Reduction
Atomic debris	He buffer gas	$>10^2\times$
Cluster debris	Tape type laser target	$\sim 10^2\times$
	or angle	$\sim 10\times$
Remaining debris	Al/C–H protective filter	$\sim 10^2\times$
	or Be protective filter	complete (~6 μm Be)

(b) Future work

Problem	Main remedy	Expected enhancement
Average x-ray power	Laser repetition rate	$\sim 10\times$ (200 Hz)
Conversion efficiency	Laser pulse energy	$\sim 10\times$
	or laser pulse modulation	$\sim 10\times$

semiconductor device manufacturing in small-scale industrial and R&D environments (*2, 3, 12*).

Further improvement is possible using more powerful, commercially available laser systems. Increase in output power of excimer lasers is a general trend, which is supported by the development of multikilowatt excimer lasers in various international projects like Eureka (*36*).

V. CONCLUSIONS

Utilizing a modern commercial KrF excimer laser as a driver we have demonstrated that it is possible to operate a laser plasma x-ray source at high repetition rates up to 40 Hz under well controlled conditions suitable for x-ray microlithography. Repetition rates of ~100 Hz are feasible.

Major drawbacks of laser plasma x-ray sources have been assessed and several solutions have been investigated with quantitative results. First, an effective reduction by over two orders of magnitude in the deposition rate of debris has been measured by applying atmospheric He buffer gas with a slow flow rate in the source chamber. Second, it has been shown that a tape laser target suppresses cluster-sized debris by two orders of magnitude at small angles relative to the target normal. These angles are preferable for exposing photo-resists because here the x-ray intensity reaches a pronounced maximum. The laser target geometry (laser incident at 45°) makes these small angles accessible. Thin, highly transparent filters are likely to provide sufficient protection to stop residual debris.

It has been demonstrated that sub-0.5-μm structures can be replicated accurately in a general purpose photo-resist, using the source at 20-Hz repetition rate and applying the investigated remedies.

A significantly cleaner x-ray source has been constructed. If in the future all investigated remedies are incorporated, this source is expected to meet the demands imposed by microlithography in an IC-production environment. A necessary condition to achieve this is that the average x-ray power be enhanced by at least two orders of magnitude to enable resist exposure to be achieved in several seconds. This is feasible using currently available commercial laser systems. More research is needed on modifying pulse properties of modern excimer lasers in order to improve the laser light-to-x-ray conversion efficiency. As a part of our present program higher efficiencies should be achieved either by reducing the pulse length or by enhancing the pulse energy.

Since laser plasma x-ray sources are generally operated at longer wavelengths than synchrotron radiation sources, separate investigations into the effect of wavelength on issues such as resolution and process latitude are desirable. Such investigations would certainly contribute to a straightforward comparison of the imaging performance of different source types.

ACKNOWLEDGMENTS

We kindly acknowledge H. Huber and H. Oertel of the Fraunhofer Institut für Mikrostrukturtechnik (Berlin, FRG) for the supply of essential x-ray masks, and R. Dammel and G. Pawlowski of Hoechst AG Corporate Research (Frankfurt, FRG) for kindly supplying photo-resist. Furthermore we acknowledge the assistance of T. Blatchford (Rutherford Appleton Laboratory) and J. Toth (Delft Institute of Microelectronics

and Submicron Technology DIMES, Delft, the Netherlands) with SEM inspection. Additional SEM inspection was done by J. van de Sanden, P. A. Veenhuizen, and A. M. Kerrigan (SKF Research Laboratory, Nieuwegein). C. Brown (Rutherford Appleton Laboratory) is acknowledged for filter manufacture. For resist characterization the clean room facilities of Rutherford Laboratory and DIMES were utilized.

This work is part of the SERC Rutherford Appleton Laboratory research programme (United Kingdom) and the research programme of FOM, the Foundation for Fundamental Research on Matter (the Netherlands). The work described is made possible by financial support from the UK Department of Trade and Industry through EUREKA, NWO (the Netherlands Organization for Scientific Research), STW (the Netherlands Technology Foundation), and the Netherlands Government in the framework of EUREKA.

REFERENCES

1. A. D. WILSON, *SPIE Conf. Proc.* **537,** 85 (1985).
2. A. HEUBERGER, *SPIE Conf. Proc.* **1089,** 140 (1989).
3. R. D. FRANKEL, J. P. DRUMHELLER, A. S. KAPLAN, AND M. J. LUBIN, *in* "Inter Face '86 Conference Proceedings, San Diego," p. 82, 1986.
4. F. O'NEILL, M. C. GOWER, I. C. E. TURCU, AND Y. OVADANO, *Appl. Opt.* **25,** 464 (1986).
5. F. O'NEILL, G. M. DAVIS, M. C. GOWER, I. C. E. TURCU, M. LAWLESS, AND M. WILLIAMS, *SPIE Conf. Proc.* **831,** 230 (1987).
6. T. TOMIE, K. KOYAMA, N. ATODA, S. KOMEIJI, Y. MATSUMOTO, A. YAOITA, I. MATSUSHIMA, AND M. YANO, *SPIE Conf. Proc.* **831,** 224 (1987).
7. M. KÜHNE AND H.-C. PETZOLD, *Appl. Opt.* **27,** 18, 3926 (1988).
8. F. BIJKERK, G. E. VAN DORSSEN, M. J. VAN DER WIEL, R. DAMMEL, AND J. LINGNAU, *Microelectr. Eng.* **9,** 121 (1989).
9. R. DAMMEL, C. R. LINDLEY, G. PAWLOWSKI, U. SCHEUNENMANN, AND J. THEIS, *SPIE Conf. Proc.* **1262,** 378 (1990).
10. F. O'NEILL, I. C. E. TURCU, D. XENAKIS, AND H. R. HUTCHINSON, *Appl. Phys. Lett.* **55,** 25, 2603 (1989).
11. I. C. E. TURCU, F. O'NEILL, G. J. TALLENTS, T. HANNON, D. BATANI, A. GIULIETTI, C. W. WHARTON, AND R. A. MELDRUM, *SPIE Conf. Proc.* **1278** 32 (1990).
12. E. CULLMANN, T. KÜNNETH, W. NEFF, AND K. H. STEPHAN, *J. Vac. Sci. Technol. B* **5,** 3, 638 (1987).
13. KANTI JAIN, "Excimer Laser Lithography," SPIE Opt. Eng. Press, Bellingham, WA, 1990.
14. D. BATANI, E. TURCU, AND G. J. TALLENTS, *SPIE Conf. Proc.* **1503,** 479 (1991).
15. B. L. HENKE, F. G. FUJIWARA, M. A. TESTER, C. H. DITTMORE, AND M. A. PALMER, *J. Opt. Soc. Am. B* **1,** 6, 828 (1984).
16. R. M. A. AZZAM AND N. M. BASHARA, "Ellipsometry and Polarized Light," p. 270, North-Holland, Amsterdam, 1987.
17. N. G. ALEXANDROPOULOS AND G. C. COHEN, *Appl. Spectrosc.* **28,** 155 (1974).
18. R. J. HUTCHEON, J. P. PYE, AND K. D. EVANS, *Astron. Astrophys.* **51,** 451 (1976).
19. U. FELDMAN, G. A. DOSCHEK, R. D. COWAN, AND L. COHEN, *J. Opt. Soc. Am.* **63,** 1445 (1973).
20. R. L. KELLY, *J. Phys. Chem. Ref. Data* **16,** Suppl. 1 (1987).
21. M. CHAKER, H. PEPIN, V. BAREAU, S. BOILY, B. LAFONTAINE, R. FABBRO, I. TOUBHANS, B. FARAL, J. F. CURRIE, D. NAGEL, AND M. PECKERAR, *SPIE Conf. Proc.* **733,** 58 (1987).
22. G. M. DAVIS, M. C. GOWER, F. O'NEILL, AND I. C. E. TURCU, *Appl. Phys. Lett.* **53,** 17, 1583 (1988).
23. R. DAMMEL, unpublished.
24. H. I. SMITH AND M. L. SCHATTENBURG, "Soft X-ray Projection Lithography, Conference Proceedings, Monterey, 1991."
25. N. ATODA AND K. HOH, *in* "Proceedings, International Symposium, VLSI Technology, Systems and Applications, Taipei, 1987," p. 48.
26. F. E. IRONS, *J. Quant. Spectrosc. Radiat. Transfer* **22,** 37 (1979).

27. Quantrad Corp., Torrance, California 90502.

28. M. L. GINTER AND T. J. MCILRATH, *Appl. Opt.* **27,** 5, 885 (1988).

29. M. BORN AND E. WOLF, "Principles of Optics," Pergamon, Elmsford, NY, 1965.

30. Some photoionization due to plasma VUV radiation is likely to take place, this will further reduce the effusion of debris from the plasma. See M. L. GINTER AND T. J. MCILLRATH, *Appl. Opt.* **27,** 5, 885 (1988).

31. J. V. ROBINSON, "Handbook of Spectroscopy," Vol. 1, CRC Press, Boca Raton, FL, 1974.

32. M. C. GOWER, *Opt. Comm.* **36,** 43 (1981).

33. I. C. E. TURCU, M. C. GOWER, C. J. REASON, P. HUNTINGTON, G. J. TALLENTS, Y. AL-HADITHI, M. SCHULZ, A. G. MICHETTE, F. BIJKERK, AND E. LOUIS, *SPIE Conf. Proc.* **1503,** 391 (1991).

34. I. C. E. TURCU, G. J. TALLENTS, M. SCHULZ, AND A. G. MICHETTE, "X-ray Microscopy," Vol. III, Springer, Berlin, New York, in press.

35. F. BIJKERK, E. LOUIS, G. E. VAN DORSSEN, AND M. J. VAN DER WIEL, *SPIE Conf. Proc.* **1089,** 274 (1989).

36. E. MÜLLER-HORSCHE, P. OESTERLIN, AND D. BASTING, *SPIE Conf. Proc.* **1503,** 28 (1991).